Zebrafish xenograft model: Identification of novel mechanisms driving prostate cancer metastasis

Chen, L.

Chapter 6

AMPK-Autophagy-dependent metabolic stress-coping machinery promotes prostate cancer metastasis

Lanpeng Chen[1#], Dionne Blangé[1#], Siddhartha Mukherjee[1], Gangyin Zhao[1], Bruno Guigas[2] and B. Ewa Snaar-Jagalska[1*]

[1] Institute of Biology, Leiden University, Leiden, Netherlands

[2] Department of parasitology, Leiden University Medical Center, Leiden, Netherlands

[#] These authors contribute equally to the manuscript

[*] Corresponding author

Prof. B. Ewa Snaar-Jagalska, b.e.snaar-jagalska@biology.leidenuniv.nl

Manuscript in preparation

Abstract

The energy sensor AMPK is a protein complex regulating cellular energy homeostasis. It protects cells from multiple stresses induced by hypo-oxidization, anoikis and energy deficiency. In cancer, AMPK serves as a tumor suppressor that inhibits cell proliferation at the early stage of the disease. Its role in the malignant stage, however, remains elusive. Our analysis of clinical datasets showed that the AMPK subunits AMPKα1 and AMPKα2 are increasingly expressed in prostate cancer metastasis and correlate with a poor prognosis in stratified high risk patients. We unveiled that AMPKα1 promotes metastasis of prostate cancer cells in 2 distinguishing manners. On one hand, AMPKα1 is required for the maintenance of stemness features of the cancer cells. On the other, AMPK mediates metabolic stress-induced cell invasion through activation of autophagy. Genetic and pharmacologic targeting of AMPK suppressed cancer cell proliferation, invasion, metastatic tumor growth, and increase cell sensitivity to mTORc1 inhibitor RAD001. Altogether, our study highlights an important role of AMPK-autophagy axis in the metastasis of prostate cancer with a clinical potential.

Introduction

Prostate cancer (PCa) is the most common cancer among men in the Netherlands in 2018 (Integraal kanker centrum Nederland (IKNL), 2018). At early stage, prostate cancer can be treated with prostatectomy and radiotherapy. However, 20%-30% of the patients who positively respond to the initial treatment still develop incurable bone metastasis, which is a main cause of prostate cancer-related death (Kelly & Yin, 2008). Metastasis is a complicated process starting from intravasation of single cancer cells/clusters at the primary site (Hanahan, &Weinberg, 2011). After circulation in blood flow, majority of the disseminated cancer cells regress due to the challenge of a series of stresses like anoikis, oxidative stress, metabolic deficiency and immuno-challenging (Moreno-Smith, Lutgendorf, & Sood, 2010). Only a small fraction of cancer cells who are capable of dealing with these stresses can survive, extravasate and eventually form metastatic growth (Hanahan, &Weinberg, 2011).

One of the cell autonomous components dealing with cellular stress is the AMPK-activated protein kinase (AMPK), a heterotrimeric serine/threonine kinase complex serving as an energy sensor. It regulates levels of ATP, ADP, and AMP in the cell. AMPK is activated by reduced ATP/ADP ratio when the cells are facing metabolic challenging (Faubert, Vincent, Poffenberger, & Jones, 2015). Consequently, the active AMPK maintains cellular energy level by inhibition of ATP-consuming processes such as translation of proteins, synthesis of cholesterol and fatty acids. In addition, the activation of AMPK also lead to autophagy, a self-eating process degrading intracellular components to preserving the levels of ATP during energy deficiency (Ke, Xu, Li, Luo, & Huang, 2018).

Autophagy is a process in which cellular components are engulfed by a double membraned autophagosome and degraded to produce energy (Mizuchima, 2007). This process is of importance for cells to cope with stresses such as nutrient deficiency, detachment from the extracellular matrix, accumulation of aggregated proteins and damaged organelles, by maintaining cellular homeostasis (Yang et al., 2013). Autophagy starts with the formation of

the phagophore, which further engulfs the cytoplasm or certain organelles in the cells forming a double membrane known as autophagosomes. Autophagosome finally fuses with lysosome and the engulfed organelles and protens are degraded by the lysosomal hydrolases (Mizuchima, 2007). Autophagy is regulated by various signaling proteins coded by autophagy-related genes (Atg) (Mizuchima, 2007). These proteins (Atg-5, Atg-12, Atg-7, Atg-10, Atg-16 and LC3) form a complex which is essential for the formation and elongation of the autophagosomal membrane (Quintanilla-Vega et al., 2014).

AMPK induces autophagy through activation of unc-51-like kinase 1 (Ulk1). After sensing low energy level in the cells, phosphorylated AMPK activates Ulk1 by a coordinated cascade in mTORC1 dependent and independent manners. In mTORC1 dependent pathway, AMPK inactivates mTORC1 through phosphorylation of TSC2 and Raptor, which further attenuates the phosphorylation of Ulk1 on Ser 757, inducing Ulk1-AMPK interaction and eventually leading to autophagy activation (Kim, Kundu, Viollet, & Guan, 2011). Apart from that, AMPK can also directly activates Ulk1 through phosphorylation of Ser 317 and Ser 777 to induce autophagy (Kim, Kundu, Viollet, & Guan, 2011).

Although the function of AMPK and autophagy in cell energy homeostasis has been well documented, it is still unclear how this energy-coping machinery controls metastatic behavior of cancer cells. Our analysis with clinical datasets showed that high expression of AMPK subunits AMPKα1 and AMPKα2 correlates with a poor prognosis and high risk of metastasis in PCa patients, implying a correlation between AMPK-autophagy-dependent energy serving and cancer malignancy. In order to identify the role of AMPK and autophagy in PCa metastasis, we injected human prostate cancer cells PC-3M-Pro4 into zebrafish embryos. Transcriptome analysis of human prostate cancer cells metastasizing in zebrafish embryos showed an up-regulation of AMPKα1/2, TSC2 and Ulk1 expression in comparison with the cells in culture. We further indicated that AMPK regulates PCa proliferation, invasion and mTOR inhibitor tolerance in autophagy-dependent manner, and CSC-like phenotype in autophagy-independent manner. Targeting of either AMPK or autophagy significantly blocked cancer cell growth, invasion, metastatic tumor initiation and mTORC1 inhibitor resistance, indicating an indispensable role of AMPK-autophagy axis in prostate cancer metastasis with a clinical potential.

Results

AMPKα1 and AMPKα2 are upregulated during metastasis in zebrafish xenografts and correlate with high metastatic risk of PCa patients

The clinical relevance of AMPK upregulation was investigated by analyzing the public clinical dataset Taylor MSKCC Prostate GSE21032, which showed that high expression of AMPKα1/2 is associated with a significantly reduced survival (Fig. 1a, hazard ratio (HR)=2.35 and p=0.01864). Next the expression of AMPKα1 in the primary site and metastasis was further compared (Taylor MSKCC Prostate GSE21032, 181 samples from primary site and 37 samples from metastasis), showing increased expression of AMPKα1 in metastases in comparison with the primary tumor (Fig. 1b). This upregulation of AMPKα1 was detected in metastases of bone, brain and lymph node (Fig. 1c).

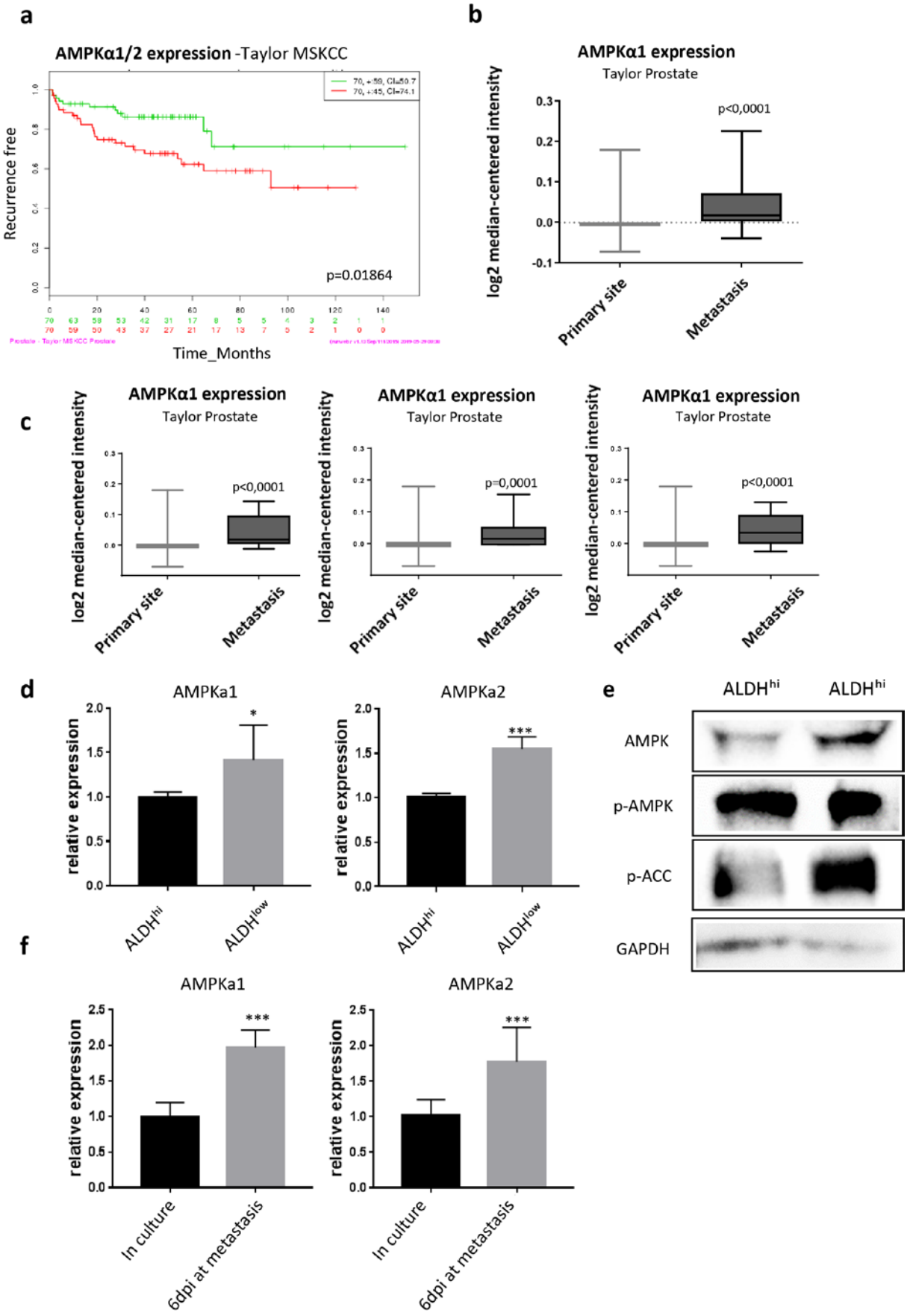
a
AMPKα1/2 expression -Taylor MSKCC
Recurrence free
p=0.01864
Time_Months
b
AMPKα1 expression
Taylor Prostate
log2 median-centered intensity
p<0,0001
Primary site
Metastasis
c
AMPKα1 expression
Taylor Prostate
log2 median-centered intensity
p<0,0001
p=0,0001
p<0,0001
Primary site
Metastasis
d
AMPKa1
AMPKa2
relative expression
ALDHhi
ALDHlow
e
ALDHhi
ALDHhi
AMPK
p-AMPK
p-ACC
GAPDH
f
AMPKa1
AMPKa2
relative expression
In culture
6dpi at metastasis

Fig. 1 AMPK is upregulated in metastasis in zebrafish xenografts correlates with poor survival and high metastatic risk of PCa patients. (a) Disease recurrence and patient survival were analyzed with Kaplan-Meier survival curve. Patients with high expression of AMPKα1 and AMPKα2 (red) have a high probability of recurrence and death compared to the low expression one (green) in clinical dataset Taylor MSKCC (p=0.01864). (b) AMPK is upregulated in prostate cancer metastasis compared with the primary site. (c) AMPK is upregulated in lymph node, bone and brain metastasis compared with the primary site (p<0.0001, p=0.0001, p<0.0001 respectively). Clinical dataset Taylor Prostate is used for the analysis (data accessed form www.oncomine.org). (d) AMPKα1 and AMPKα2 expression is increased in $ALDH^{hi}$ compared to $ALDH^{low}$. n=3. (e) $ALDH^{hi}$ has increased protein levels of AMPK, p-AMPK and p-ACC compared to $ALDH^{low}$. (f) Engrafted PC-3M-Pro4 in zebrafish metastases at 6dpi has enhanced expression of AMPKα1 and AMPKα2 in comparison with the cells in culture. n=3.

Considering that the cell subpopulation with high ALDH has been identified as a CSC-enriched subpopulation which harbors enhanced metastatic capacity in both ZF and mice xenografts (Chen et al., 2019, Van Den Hoogen et al., 2010) we measured the expression (Fig. 1d) and activation (Fig. 1e) of AMPK in the $ALDH^{hi}$ subpopulation isolated from PC-3M-Pro4. Consequently, both expression and phosphorylation of AMPKα1 in $ALDH^{hi}$ were increased in concert with elevated phosphorylation of AMPK downstream Acetyl-CoA carboxylase (ACC) when compared to $ALDH^{low}$ (Fig. 1e), indicating $ALDH^{hi}$ cell subtype had an increasing activation of AMPK signaling pathway.

We next analyzed the expression of AMPK in the cancer cells during metastasis. When PC-3M-Pro4 was intravenously injected into 2 days old ZF, distant metastases were developed around the hematopoietic niche within 6 days. Transcriptomic of the cancer cells in zebrafish metastases at 6 days post injection (6dpi) were analyzed and compared with the cancer cells in culture. The result showed an upregulation AMPKα1/2 in the experimental metastases (Fig. 1f) while the gene sets for glycolysis, TCA cycle, carbon metabolism and mTORC1 signaling were downregulated (Fig. S1). Altogether, this data indicates that the cancer cells are facing sever metabolic challenge during the experimental metastatic tumor growth and AMPK signaling is upregulated to cope with the stress.

Active AMPK mediates starvation-induced cancer cell invasion

In order to study responses of cancer cells to metabolic stress *in vitro*, PC-3M-Pro4 was cultured in the basic medium containing 10%, 5%, 2.5% or 0.5% serum. Analysis by western blot showed that the depletion of serum in the medium caused an increase of AMPK expression and phosphorylation (Fig. 2a). Moreover, this serum depletion also enhanced the phosphorylation of Ulk-1 on Ser555 and the production of LC3, indicating an activation of the autophagy cascade (Fig. 2a).

To study the cell responses to the serum depletion in a 3D environment, PC-3M-Pro4 tumor spheroids were embedded into type-I collagen. The number of cells that invaded into the neighboring space from the central mass was counted. Surprisingly, the serum depletion led to a significantly increased cell invasive phenotype in a dose dependent manner. The cells in 0.5% serum had the strongest invasive phenotype at 2 dpi (Fig. 2b).

AMPK is part of an energy-sensing pathway which conserves cellular energy in case of energy deficiency (Faubert et al., 2015). Therefore we detected if the activation of AMPK contributes

to the serum depletion promotes cancer cell invasion. PC-3M-Pro4 cells embedded in type-I collagen were treated with AMPK activator 991 in the medium containing 10% serum. This 991 treatment significantly increased the invasive phenotype of the cancer cells, indicating that AMPK activation is functionally involved in the starvation-induced cancer cell invasion (Fig. 2c).

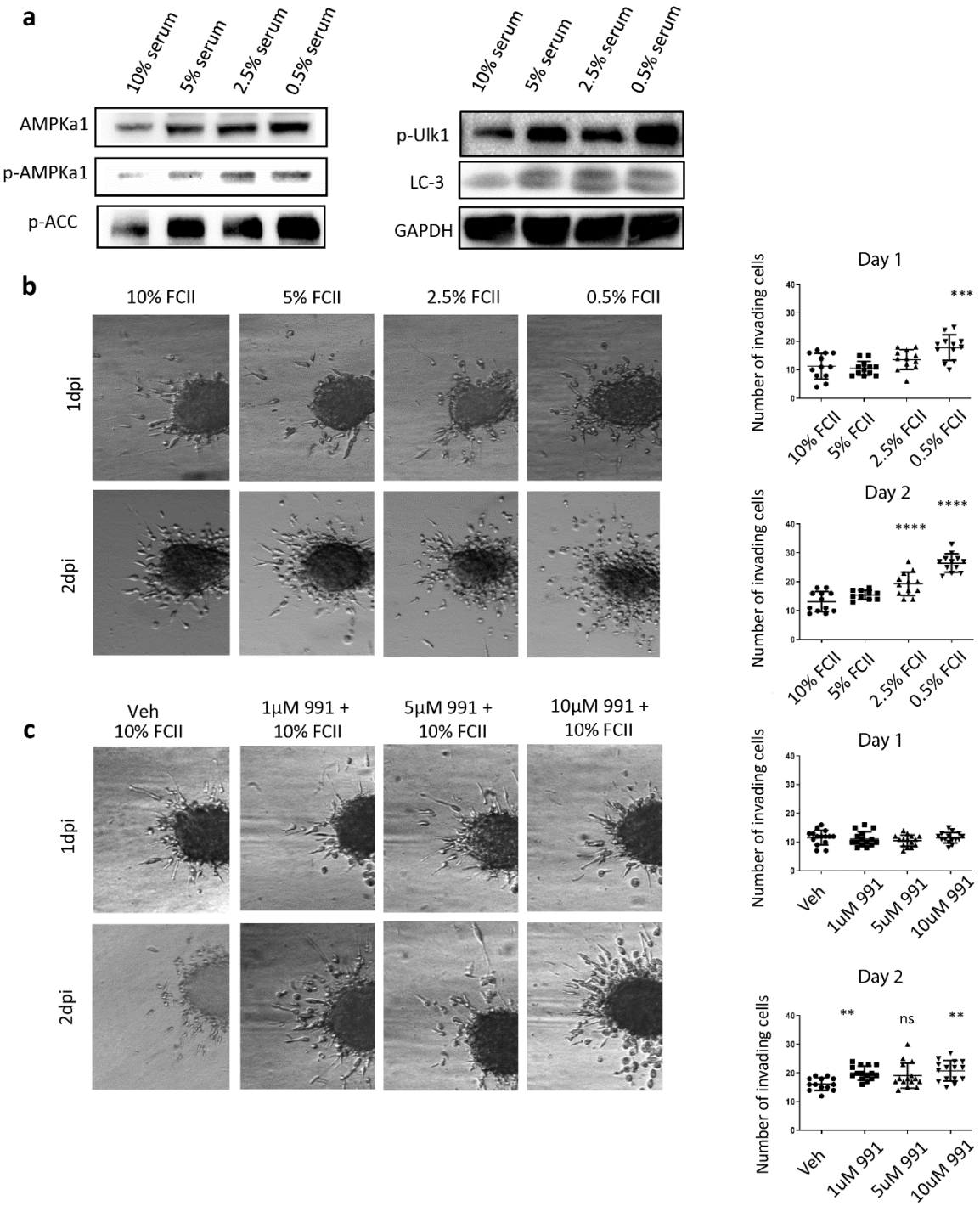

Fig. 2 Serum depletion enhances cancer cell 3D invasion through activation of AMPK (a) Starvation treatment enhanced phosphorylation of AMPK, ACC, Ulk1 and increased accumulation of LC-3. (b) PC-3M-Pro4 cells were

embedded in 1mg/ml collagen type I covered with medium containing different concentrations of serum. Decrease of serum concentration significantly increased the number of invading cells ($p<0.0001$, $n=15$). (c) AMPK activator 991 significantly increased the number of invading cells in 1mg/ml collagen type I covered with medium containing 10% FCS($p=0.0033$, $n=15$).

AMPKα1 knockdown suppresses the expression of pluripotency genes, clonogenicity and proliferation

Next we assessed the role of AMPKα in governing cancer cell aggressiveness using RNAi interference approach in PC-3M-Pro4 cells. The efficiency of the knockdowns was validated by qPCR (Fig. 3a). Both AMPKα1 and AMPKα2 knockdowns significantly decreased AMPK expression. Compared with the AMPKα2 knockdowns, which only suppressed AMPKα2 expression, AMPKα1 knockdowns inhibited the expression of both AMPKα1 and AMPKα2 and were therefore considered as double knockdown. Furthermore, expression of CSC markers, Nanog, Oct4 and Sox2, was measured in the AMPKα1 knockdown cells. It showed that the expression of Nanog and Oct4 was significantly decreased by the knockdowns (Fig. 3b). The self-renewal capacity of the cancer cells was measured by a clonogenicity assay. AMPKα1 knockdowns significantly suppressed the size of colonies formed by single cancer cells (Fig. 3c). In cell proliferation assay, AMPKα1 knockdowns also significantly suppressed the proliferation when the cells were grown in medium with 10% of serum (Fig. 3d). Taken together, our knockdown studies revealed that the expression of AMPKα1 is important for the maintenance of pluripotency gene expression, and promotes clonogenicity and proliferation of the PCa cells.

The role of AMPK in cell responses to serum depletion was assessed using the AMPK kd cells (Fig. 3e). After serum depletion, both total protein level and phosphorylation of AMPK were suppressed by both knockdowns. These knockdowns inhibited the starvation-induced phosphorylation of Ulk-1 and accumulation of LC3, indicating AMPK mediates the energetic deficiency-induced autophagy. ACC, on the other hand, was increased in both knockdowns, suggesting a presence of an alternative, AMPK-independent pathway to control fatty acid synthesis. In 3D invasion assay, the cell invasive phenotype was significantly suppressed by both AMPKα1 knockdowns (Fig. 3f). Overall, these results indicated that AMPKα1 mediates autophagy and 3D invasion of the PCa cells in response to the energy deficiency.

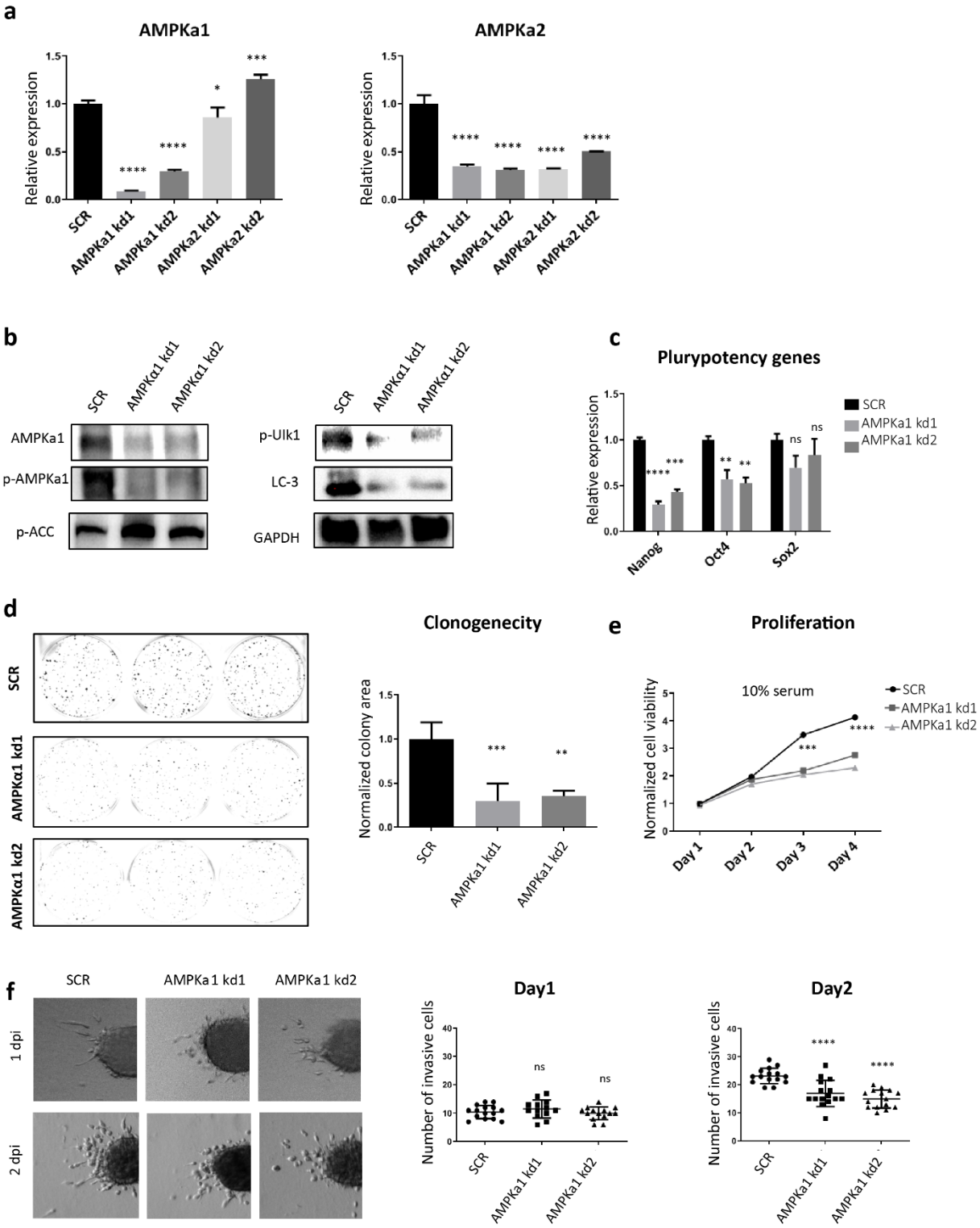

Fig. 3 AMPKα1 knockdown suppresses the pluripotency gene expression, clonogenicity, proliferation and starvation-induced 3D invasion. (a) AMPKα1 and AMPKα2 knockdown in PC-3M-Pro4 was validated by qPCR. AMPKα1 knockdown suppressed the expression of both AMPKα1 and AMPKα2 ($p<0.0001$), while AMPKα2 knockdown only suppressed the expression of AMPKα2 ($p<0.0001$). (b) Knockdown of AMPK α1 suppressed phosphorylation of AMPK and Ulk1, and decreased accumulation of LC-3. (c) Nanog and Oct4 mRNA level was significantly inhibited by AMPKα1 kd1 and kd2 ($p<0.01$, n=3). (d-e) Clonogenicity and proliferation of PC-3M-Pro4 were significantly inhibited by AMPKα1 kd1 and kd2 ($p=0.0002$, n=3). (f) AMPKα1 knockdown significantly suppressed 3D invasion of PC-3M-Pro4 in the medium containing 2.5% serum ($p<0.0001$, n=15).

AMPKα1 knockdown inhibits metastatic tumor growth of prostate cancer in zebrafish xenografts

Next we tested the effect of AMPK interference on the metastatic capacity of the cancer cells. We intravenously injected PC-3M-Pro4 containing the non-targeted control (SCR), AMPKα1 kd1 and AMPKα1 kd2 in zebrafish embryos. The total cancer cell burden at the metastatic site (CHT) was measured at 1, 4 and 6dpi. At 1dpi, the cancer cell burden of SCR control, AMPK kd1 and AMPK kd2 cells were similar. At 4 and 6dpi, however, the knockdowns of AMPKa1 significantly inhibited cancer cell growth at the metastatic site (Fig. 4a-b), demonstrating an essential role of AMPK signaling in governing PCa metastatic tumorigenicity.

AMPKα1 promotes cancer cell clonogenicity and invasion through induction of autophagy

Subsequently , we detected if AMPK regulates cancer cell aggressiveness through inducing autophagy. Considering AMPK induces autophagy through activation of Ulk1 (Kim, Kundu, Viollet, & Guan, 2011), we performed RNAi interference to knockdown the expression of Ulk-1 to suppress AMPK induced autophagy (Fig. 5a). The effect of Ulk-1 knockdowns on autophagy was validated by westernblot. The accumulation of LC3 was, however, was only efficiently inhibited by Ulk-1 kd2 (Fig. 5b), indicating that ULK-1 kd2 but not kd1 is effective to suppress autophagy.

Next we detected the effect of Ulk-1 knockdowns on pluripotency gene expression, and showed that the expression was not affected by the knockdown (Fig. 5c). This data suggested that AMPK controlled CSC-like phenotype independent from autophagy. In clonogenicity assay, consistent with the AMPK knockdowns, Ulk-1 kd2 but not Ulk-1 kd1 significantly suppressed the size of colonies (Fig. 5d). To further confirm if the Ulk-1 knockdown suppressed clonogenicity via inhibition of autophagy, we generated ATG-5 knockdowns, which significantly suppressed the formation of colonies (Fig. 5d), indicating autophagy is indeed required for cell clonal growth. Next, we detected if the genetic interference of autophagy affected the starvation-induced cell invasion. Surprisingly,Ulk-1 knockdown did not suppressed cell invasion in 2.5% serum medium, although the invasive phenotype was significantly suppressed by ATG-5 knockdown (Fig. 5e). This discrepancy can be explained by the fact that the Ulk-1 kd was not sufficient to totally block the starvation-induced autophagy, which could still promoted the invasive phenotype.

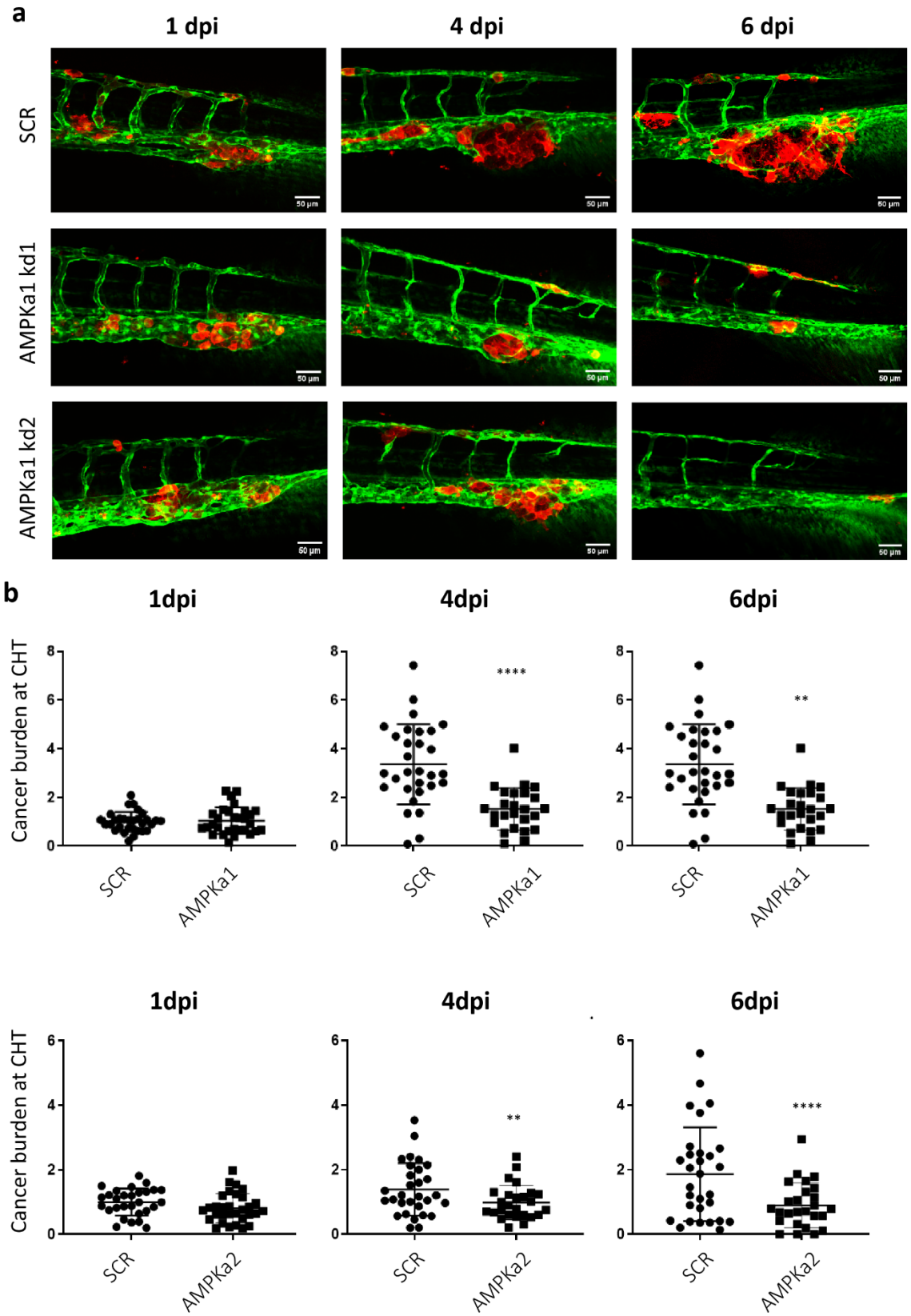

Fig. 4 AMPKα1 knockdown inhibits metastatic spreading of prostate cancer cells *in vivo.* (a-b) PC-3M-Pro4-mCherry bearing SCR, AMPKα1 kd1 and AMPKα1 kd2 into zebrafish embryos at 2dpi. Both AMPK α1 knockdowns significantly inhibited metastatic growth of the cancer cells around CHT at 4 and 6 dpi (n=30, p<0,01).

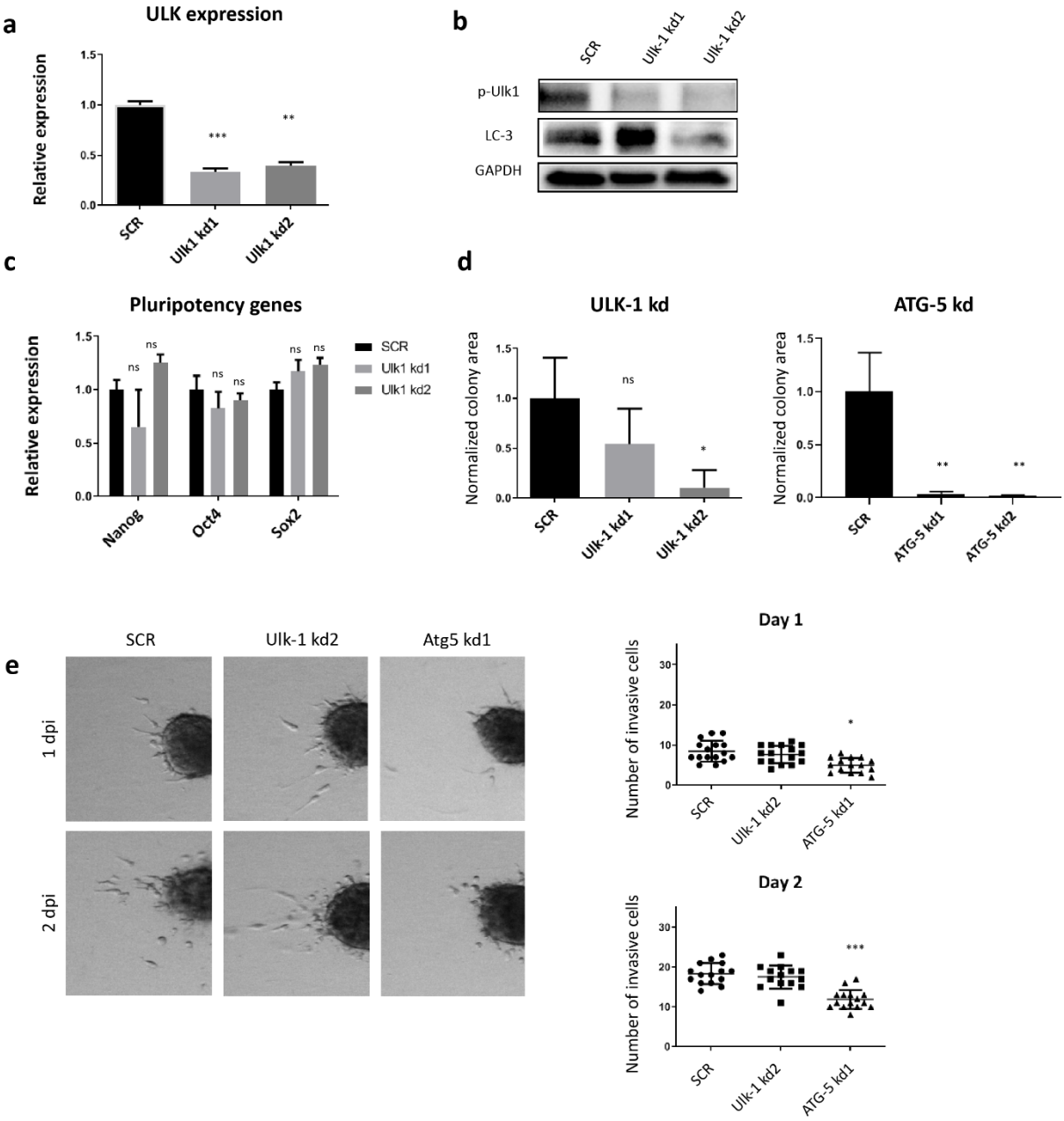

Fig. 5 Genetic targeting of autophagy suppresses clonogenicity and proliferation. (a) Efficiency of Ulk-1 knockdown in PC-3M-Pro4 was validated in vitro by qPCR. Ulk-1 expression was significantly suppressed by both knockdowns ($p<0.01$). (b) The effect of Ulk-1 kd on autophagy was validated by western blot. Ulk-1 kd2 showed stronger inhibitory effects on p-Ulk and LC3 on protein level. (c) Both Ulk-1 knockdowns did not affect the expression of pluripotency genes ($p=0.1$, $n=3$). (d) The clonal growth was significantly inhibited by ULK-1 kd2 and ATG-5 kd1 and ATG-5 kd2 ($p=0.0423$, $n=3$). (e) Atg5 knockdown significantly inhibited 3D invasion in the medium containing 2.5% serum ($p<0.0001$, $n=15$).

Suppression of autophagy inhibits metastatic tumor growth in zebrafish xenografts

To further elucidate whether AMPK drives PCa cell metastasis through the induction of autophagy, PC-3M-Pro4 cells containing the non-targeted control (SCR), ULK-1 kd cells and ATG-5 kd cells were intravenously injected into zebrafish embryos. Again, the total cancer cell burden at the metastatic site (CHT) was measured at 1, 4 and 6dpi. At 1 and 4 dpi, the cancer cell burden of SCR control and ULK-1 kd cells were similar. However, at 6 dpi, the cells bearing

ULK-1 kd2, ATG-5 kd1 and ATG-5 kd2 had significantly reduced cancer cell burden at the metastatic site (Fig. 6a-b). This data indicated that the activation of autophagy was of importance for the experimental metastatic tumor outgrowth.

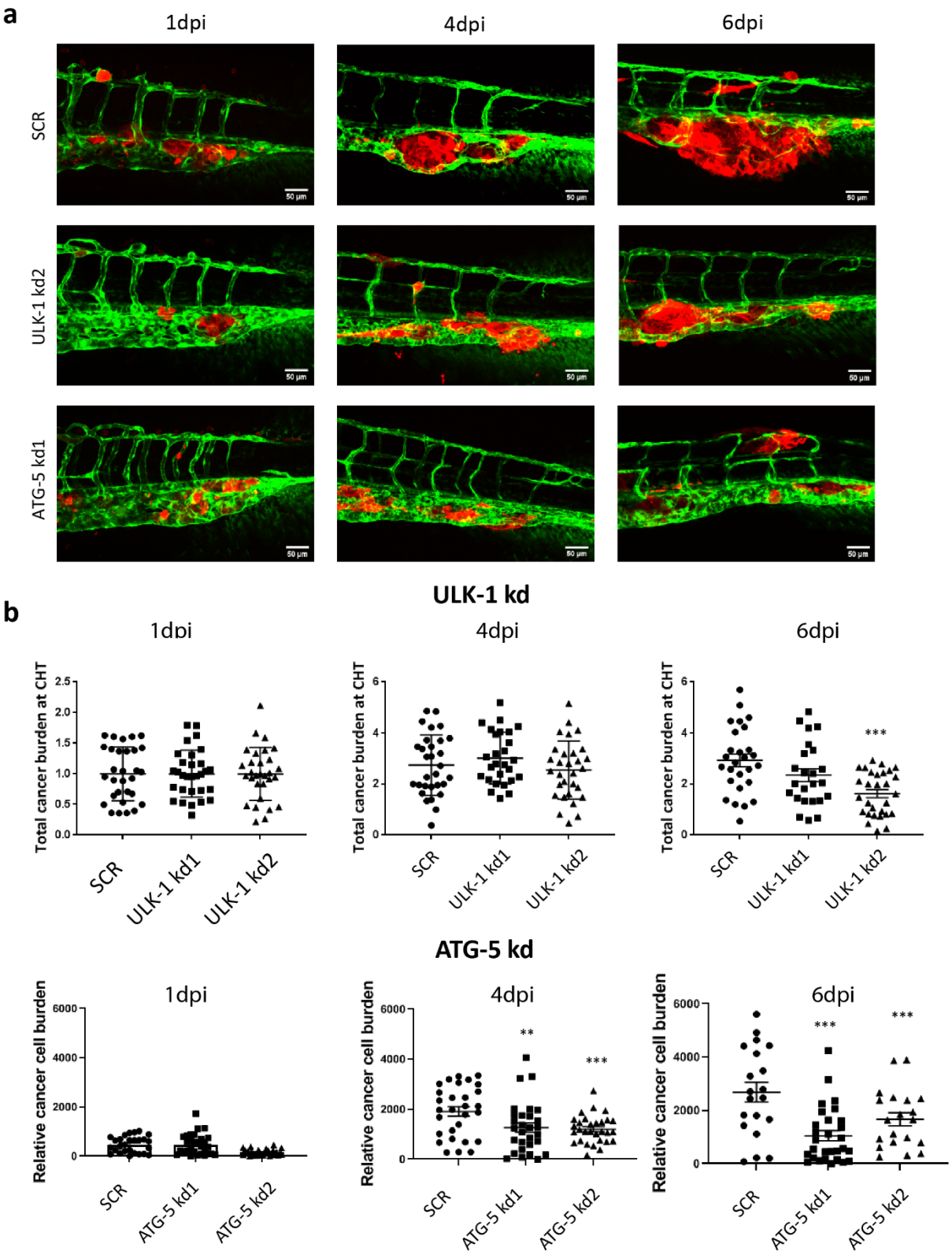

Fig. 6 ULK1 and ATG-5 knockdowns inhibit metastatic tumorigenicity of prostate cancer cells *in vivo.* (a-b) Ulk-1 kd2, ATG-5 kd1 and ATG-5 kd2 significantly inhibited metastatic growth of PC-3M-Pro4 at CHT area of zebrafish embryos at 6 dpi (n=30, $p<0.01$), indicating the importance of autophagy for metastatic tumorigenicity.

Targeting of AMPK and autophagy using chemical inhibitors suppresses PCa cell growth and invasion

Finally, we tested if targeting of AMPK-autophagy axis can be a potential approach against PCa cell growth. We therefore treated cancer cells with AMPK inhibitor compound C and autophagy inhibitor chloroquine (CQ) (Kabeya, 2004). The cell viability of PC-3M-Pro4 cells was analyzed using WST assay 72 hours after the treatments. Both Compound C and CQ dramatically decreased the cell proliferation at a concentration of 5µM (Fig. 7a). Next, we measured if Compound C and CQ treatment inhibited cell growth through targeting of cell cycle using fluorescence ubiquitination cell cycle indicator (FUCCI) system, which labels cell cycle with RFP at G0/G1 phase and with GFP at S/G2/M. Result showed that both inhibitors increased the amount of cells positioned in the G0/G1 phase (Fig. 7b), suggesting treatment induced cell cycle arrest at G1 checkpoint. In the end, the effect of the compounds on starvation-induced cell invasion was assessed. Treatments with either Compound C or CQ significantly inhibited the invasive phenotype, in basic medium containing 10% or 2.5% serum (Fig. 7c). Overall, our preliminary results suggest that chemical inhibition of AMPK and autophagy may suppress PCa cell aggressiveness.

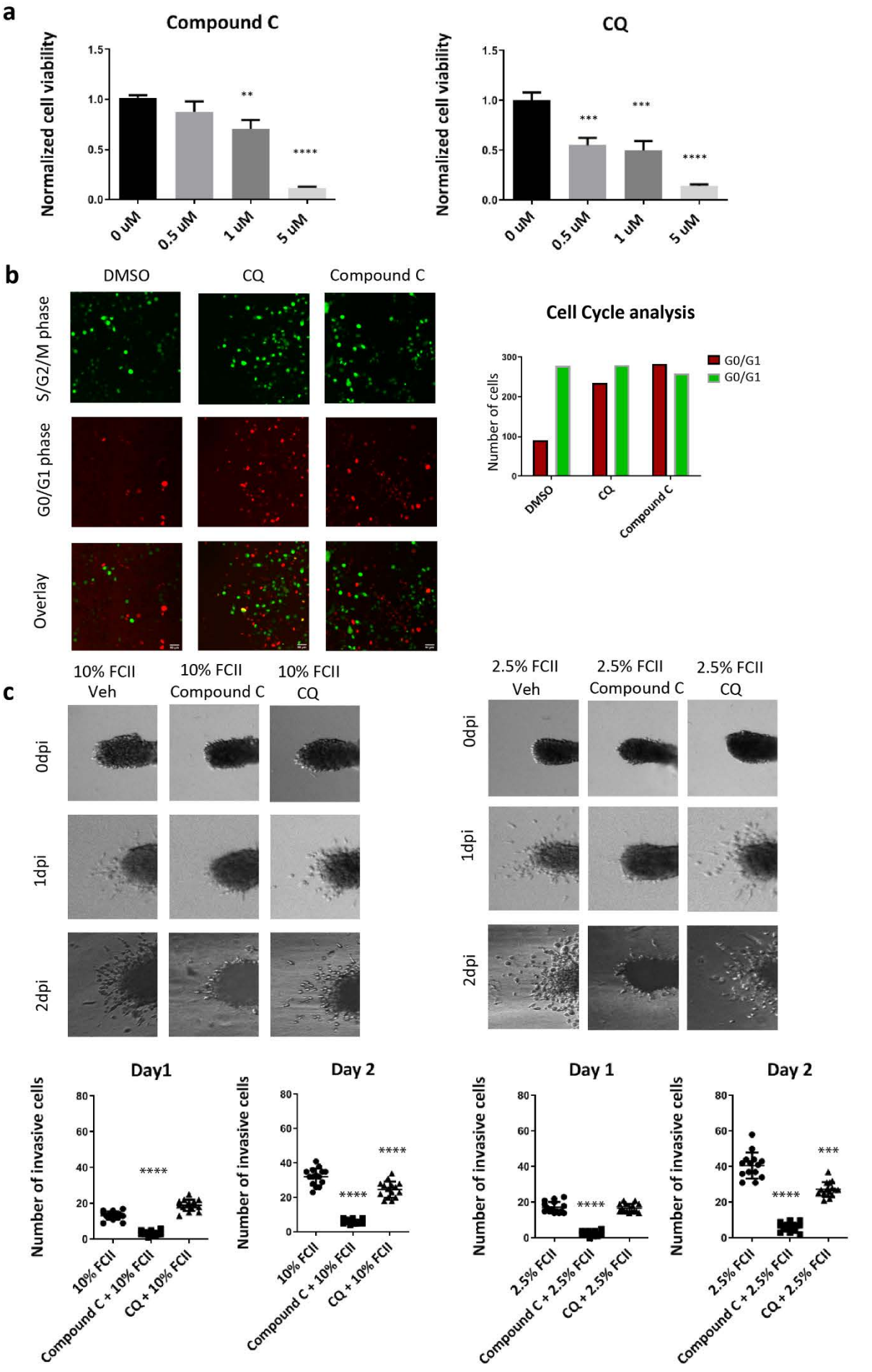
a
Compound C
Normalized cell viability
1.5
1.0
0.5
0.0
**
****
0 uM
0.5 uM
1 uM
5 uM
CQ
Normalized cell viability
***
***
****
b
DMSO
CQ
Compound C
S/G2/M phase
G0/G1 phase
Overlay
Cell Cycle analysis
Number of cells
300
200
100
0
G0/G1
G0/G1
DMSO
CQ
Compound C
c
10% FCII Veh
10% FCII Compound C
10% FCII CQ
2.5% FCII Veh
2.5% FCII Compound C
2.5% FCII CQ
0dpi
1dpi
2dpi
Day1
Day 2
Day 1
Day 2
Number of invasive cells
80
60
40
20
0
****
****
***
10% FCII
Compound C + 10% FCII
CQ + 10% FCII
2.5% FCII
Compound C + 2.5% FCII
CQ + 2.5% FCII

Fig. 7 Targeting of AMPK-autophagy signaling with inhibitors decreases proliferation and invasion of PCa cells. (a) Compound C and CQ treatments in PC-3M-Pro4 significantly decreased cell proliferation ($p<0.0001$, n=3). (b) Compound C and CQ arrested the cell cycle at G1 phase ($p<0.0001$). (c) Compound C and CQ significantly decreased the number of invasive cells in 10% and 2.5% of serum medium. ($p<0.0001$, n=15).

Synergetic targeting of mTORC1 and autophagy has stronger inhibitory effect on cell growth than single targeting

MTORC1 inhibitor RAD001 has been utilized to inhibit multiple types of cancer including PCa, however acquired drug resistance can still develop (Statz, Sara, Oatterson, & Susan, 2017). We hypothesize that the mTORC1 resistance can be induced by the activation of AMPK-autophagy axis and synergetic targeting of both mTORC1 and autophagy pathways may therefore have a stronger inhibitory effect. We therefore treated the cancer cells with RAD001 in the presence or absence of CQ (Fig. 8a-b). Although Rad001 alone inhibited the growth of PC-3M-Pro4 by 40% at the concentration of 1, 5 and 10 uM (Fig. 8a), the combination of 1uM CQ with 1, 5, or 10 uM of Rad001 significantly inhibited PC-3M-Pro4 by 80%. For C4-2B, although, the cell viability was not affected by CQ treatment, the combination of 1uM CQ with 10uM RAD001 had stronger inhibitory effect than Rad001 alone at the same concentration (Fig. 8b). Collectively, this data indicates that the synergetic targeting of mTORC1 and autophagy has stronger inhibitory effect on PCa cell growth and could be therefore considered as a potential clinical approach against PCa (Fig. 8c).

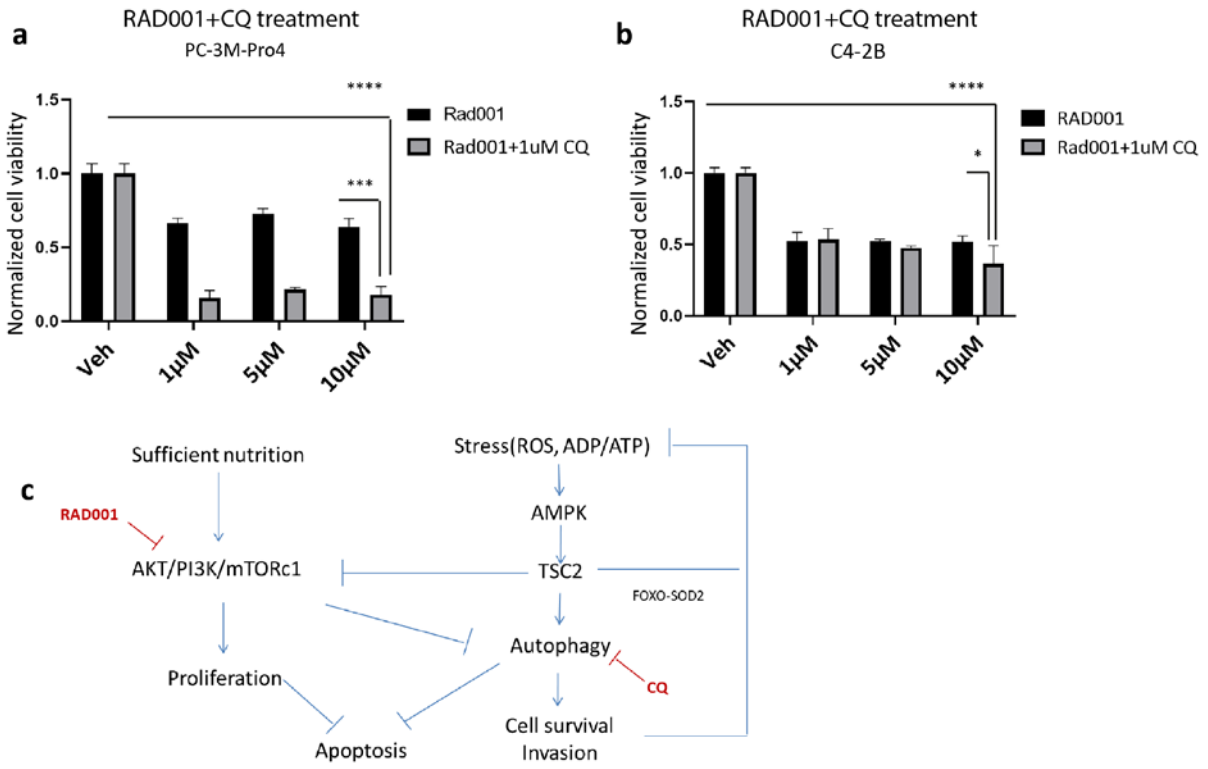

Fig. 8 Synergetic targeting of mTORC1 and autophagy has stronger inhibitory effect on cell growth than single inhibition. (a-b) Synergetic treatment using 1uM CQ with 1, 5 or 10 uM RAD001 had significantly stronger inhibitory effect than single RAD001 treatment on PC-3M-Pro4 and C4-2B. n=3. (c) Graphic indication Synergetic targeting of mTORC1 and autophagy signaling pathway. When cancer cells were challenged by low energy or mTOC1 inhibition, AMPK-autophagy axis was activated,protecting cells from stress-induced cell death and

promoted invasion. Synergetic targeting of both mTOC1 and autophagy can therefore have enhanced inhibitory effect.

Discussion

Energy sensor AMPK is activated to cope with energy deficiency by conserving cellular energy. (Faubert et al., 2015). In this research, we dissected the essential role of AMPKα1 in stimulating PCa metastasis in two distinct manners: by maintaining cancer stemness and inducing autophagy, which promote cancer cell survival, invasion and long-term proliferation.

Metastasis is a complex and inefficient process, in which only a few percent of cells that survive the stresses from the metastatic cascades such as anaoikis, shear stress, high oxidative environment and energy deficiency can develop metastases (Moreno-Smith, Lutgendorf, & Sood, 2010).

As a key stress coper, AMPK regulates cell proliferation and survival. Our experimental data shows that AMPKα1 and α2 were upregulated at the early stage of experimental metastasis in zebrafish (ZF) in concert with an enhancement of gene signatures for cell stress coping, starvation and autophagy and decrease of metabolic pathway (Fig. S1). This increased AMPKα expression is in line with the analysis of clinical dataset, which shows a correlation between AMPKα1 and α2 upregulation and PCa metastasis suggesting that AMPK can play an essential role in metastasis development (Fig. 8c).

In addition, we found that the expression and phosphorylation of AMPKα and its target ACC were significantly enhanced in $ALDH^{hi}$ CSC-enriched cell subpopulation. The importance of AMPK for the CSC maintenance was investigated by studies using AMPKα1 kd cells. AMPKα1 kd significantly decreased the expression of pluripotency genes Nanog and Oct4, self-renewal capacity and clonal growth. This CSC regulation by AMPK was autophagy independent since the knockdown of ULK-1 did not affect the expression of pluripotency genes. Considering that AMPK can phosphorylate and activate Forkhead box transcription factor 3 (FOXO3), a transcriptional factor regulating stem cell homeostasis {Tothova, 2007 #2030}, it can be further addressed if the inhibitory effect of AMPK silencing on PCa cancer stemness is due to the reduction of FOXO3 activation**.**

We subsequently analyzed if AMPK mediates cell responses to energy deficiency through regulation of autophagy. PC-3M-Pro4 was cultured in basic medium containing 10%, 5%, 2.5% or 0.5% serum. The decreasing concentrations of serum enhanced expression and phosphorylation of AMPK, phosphorylation of Ulk1 and accumulation of LC-3II, indicating an activation of AMPK-autophagy cascade by the serum depletion. Importantly, this serum depletion and AMPK activation promoted a cell invasive phenotype. Activation of AMPK by either starvation or treatment with AMPK activator 991 significantly increased the amount of invading cancer in completed medium. The knockdown of AMPK α1, on the other hand, decreased the invasive phenotype. We further demonstrated that AMPK regulates cell invasion through autophagy. Targeting of either autophagosome elongation by ATG-5 knockdown or autophagosome maturation by CQ treatment significantly inhibited the starvation-induced cell invasion in PC-3M-Pro4. Moreover the effect of Ulk-1 knockdown on cell invasion was also tested. Unexpectedly, 3D invasion was not significantly suppressed by the Ulk-1 knockdown. This discrepancy might be due to the inefficient knockdown since

certain level of Ulk-1 phosphorylation and LC-3 accumulation still remained after introduction of Ulk-1 kd. The role of AMPK-autophagy axis in metastasis was assessed in vivo using ZF xenograft model. The knockdown of AMPKα1, Ulk-1 and ATG-5 significantly inhibited metastatic tumorigenicity, highlighting the importance of the AMPK-autophagy-dependent stress-coping machinery in metastatic process.

We also investigated the clinical potential of targeting AMPK and autophagy axis. The mTORC1 inhibitors have been used in the clinic as an anti-cancer drug. However, the efficacy is still poor due to acquired resistance (Statz, Sara, Oatterson, & Susan, 2017). We hereby hypothesized that this resistance was induced due to the activation of AMPK-autophagy axis, which allows the cells to survive the treatment (Zachari & Ganley, 2017). Indeed, mTORC1 inhibitor RAD001 had relatively low inhibitory effect on PC-3M-Pro4. In contrast, the treatment with Compound C significantly decreased cell proliferation in both PC-3M-Pro4 and C4-2B. Notably, Compound C can inhibits several other kinases next to AMPK (Dasgupta & Seibel, 2018) and it is uncertain if its inhibitory effects on cell growth is partially due to the off-targets. Therefore the autophagy inhibitor CQ was tested. CQ treatment significantly inhibited cell proliferation and arrested the cell cycle in G0/G1 phase. In addition, co-treatment of the cancer cells with CQ and Rad001 together significantly inhibited the cell proliferation more potently then treatment with CQ or Rad001 alone, indicating that synergetic targeting of mTORC1 and autophagy is an efficient manner to reduce the cell proliferation rate.

In conclusion, in this preliminary study we show that human prostate cancer cells in zebrafish metastases display increased AMPK expression, which is required for stemness maintenance, invasion and proliferation, via autophagy-dependent and independent pathways. Targeting of these signaling cascades could be an effective approach to suppress metastatic tumorigenicity of prostate cancer. In future, to validate the clinical potential of this research, the effect of AMPK and autophagy inhibitors on metastasis should be confirmed in more near patient models including patients-derived xenografts and organoids.

Materials and methods

Analysis of publicly available dataset of prostate cancer patients

Gene expression based recurrence analysis was performed with SurvExpress, an online biomarker validation tool (http://bioinformatica.mty.itesm.mx/SurvExpress) (Martı et al., 2013). Gene expression between primary site and metastasis was extracted with Oncomine (Compendia Bioscience, Waltham, MA, USA).

Cell lines and cell culture

Human embryonic kidney cells HEK-293T (provided by Dr. Sylvia Le Dévédec, LACDR, Leiden) were maintained in Dulbecco's modified Eagle's medium (DMEM) supplemented with 10% FCS. Human PCa cell lines PC-3 and PC-3M-Pro4-luc2 are kindly provided by Dr. Gabriel van der Pluijm, Department of Urology, LUMC. PC-3 were cultured in Dulbecco's Modified Eagle Medium: Nutrient Mixture F-12 (DMEM/F-12) Media (Gibco^{TM}) supplemented with 10% FCS and L-glutamine. PC-3M-Pro4 were maintained in DMEM supplemented with 10% FetalCIone II (Hyclone™). C4-2B were maintained in low-glucose DMEM (Gibco^{TM}) supplemented with

20% Ham's F-12K (Sigma), 10% FCS, 1x ITS Liquid Media Supplement (Thermo Fisher Scientific), 13.6pg/ml T3, 0.25ug/ml Biotin and 25ug/ml Adenine.

Cell viability and combination treatment assay

The relative cell number was measured with Trypan Blue staining. 50% dilution of PC-3M-Pro4/C4-2B cell suspension, kept in T25 flask in 37°C incubation, was made by mixing 10µl of cells and 10µl of Trypan Blue solution. The mixture was then put into a measuring/cell-count slide (BIO-RAD) and cell number was measured using TC10 Automated Cell Counter (BIO-RAD). After cell-count, the cells were first diluted with DMEM containing 10% FC-II to reduce cell concentration to $6x10^4$ cells/ml. The cells were seeded afterwards into a 96-well plate with $6x10^3$ cells per well (100µl cell suspension per well). After 24h of incubation in 37°C, the medium was replaced with low serum medium (0.5% serum) or complete medium containing either Vehicle (Veh) control, AMPK activator 991 (kindly provided by Dr. Bruno Guigas, Department of Parasitology, Leiden), AMPK inhibitor Compound C (Sigma-Aldrich, Germany), mTORC1 inhibitor Rad001 (Sigma-Aldrich, Germany) and/or autophagy inhibitor Chloroquine (CQ) (Sigma-Aldrich, Germany). The cells were allowed to grow for 24, 48, 72 and/or 96 hours. For measurement, 10µl WST-1/well was added followed by 2 hours of incubation at 37°C. Each condition was repeated multiple times. Measurement was performed with cell plate reader TECAN Infinite M1000.

Cell cycle analysis

Ten thousand cells were seeded in an 8 wells cover chamber as described above. After 24h of incubation in 37°C, the medium was replaced with 2.5% serum medium containing 1µM CQ, 2.5µM Compound C or their combination. The cells were allowed to grow for 24 hours. The cells were imaged using Leica Confocal Microscope and the number of cells in G0/G1 phase and S/G2/M was counted using ImageJ (Rueden et al., 2017).

RNA extraction and qPCR

Cells were collected in a 15ml tube and centrifuged at 8000 rpm for 5 minutes. The supernatant was removed and the cells were stored in 500µL TRIzol (Sigma) at -20˚C. The whole process was finished within 30 minutes. RNA was isolated using the RNeasy mini kit (Qiagen) following the manufacturer's protocol. For cDNA synthesis and qPCR, iScript™ cDNA Synthesis Kit (Bio-Rad) and iQ™ SYBR® Green Supermix (Bio-Rad) were used following the manufacturer's protocol. For each gene analyzed, human specific primers were designed to measure the gene expression variation in human cancer cells. GAPDH was included as housekeeping for normalization.

Protein isolation and Western Blotting

PC-3M-Pro4/C4-2B cells were seeded in a 6-well plate and serum starved (DMEM + 2.5% FC-II) for 24h. 0.1% DMSO was used as control. 1 µM of both Rad001 and CQ, 2.5 µM of Compound C and combinations of the inhibitors (Compound C + Rad001, Compound C + CQ, Compound C + Rad001 + CQ, Rad001 + CQ) keeping the concentrations for Compound C, Rad001 and CQ 2.5, 1 and 1 µM respectively, were added to the cell medium for 24 hours. Whole-cell lysates were prepared by adding *90* µl of 10x lysis buffer diluted with 1x PBS,

supplemented with protease inhibitor (PVSF) (Sigma-Aldrich) to each well of a 6-well plate. All tubes were centrifuged at 13,200 rpm for 10 min at 4°C, and the supernatant was stored at −20°C. Protein yield was quantified using the BCA Protein Assay Kit II (Bio-Vision, Milpitas, CA, USA).

Total protein lysates (10–30 mg) were denatured in 1x TGS buffer separated by electrophoresis on a Bio-Rad Precast gel (10 or 12.5%) and transferred to polyvinylidene difluoride membranes (Millipore). The membrane was subsequently incubated with the primary antibody (**Appendix 3**) in 5% BSA in Tris-buffered saline/Tween 20 (TBST) overnight at 4°C on a roller bench. After 3 washes in TBST, the membranes were incubated with the secondary antibody (3 µl anti-rabbit or anti-mouse IgG in 3000 µl blocking buffer contains 5% BSA in Tris-buffered saline/Tween 20 (TBST)) for 1h, at room temperature as appropriate. Immunodetection was performed using the ECL Western Blot Analysis System (GE Healthcare) followed by autoradiography of the immunoblots by Gel-Doc system (Bio-Rad Laboratories, CA, USA).

3D collagen invasion assay

Collagen gel was prepared from collagen type I stock (BD, Bioscience) with a final concentration of 1 mg/ml in 44 mM NaHCO3, 0.1 M Hepes (BD, Bioscience), and 1× pen/strep (Gibco™) in DMEM medium. One mL of collagen type I mixture was added per well of a 6 wells plate and incubated at 37ºC in order to solidify. The cancer cell suspension was loaded into borosilicate glass capillary needles (1mm O.D. x 0.78mm I.D.; Harvard Apparatus) and injected in the collagen using an air-driven microinjector (20 psi, PC820 Pneumatic PicoPump; World precision Inc). Approximately 500 cells were injected. Afterwards, 2mL DMEM + FCII was added and the 6 wells plate was incubated at 37ºC. Tumor spheres were imaged at 0, 1 and 2 days past injection with Leica M165C stereomicroscope and the number of invasive cells was counted with ImageJ (Rueden et al., 2017); 10-15 tumor spheres were measured in each condition.

Clonogenicity assay

Single cells were seeded in a 6 wells plate (300 cells/well) and covered with 2mL completed medium. After 14 days, the cells were stained with crystal violet following fixation with 4% Paraformaldehyde (PFA). After imaging, size of the colonies per well were determined through ImageJ data analysis. Each experiment was independently repeated 2 times.

ALDEFLUOR assay and FACS sorting

Aldehyde dehydrogenase (ALDH) activity of the cells was measured using ALDEFLUOR Assay kit (StemCell Technology) following the manufacturer's protocol. Flow cytometric (FACS) measurement and sorting were performed on 1-10 million PC-3M-Pro4 cells treated with the ALDEFLUOR reagent. As a negative control, 500.000 cells were first treated with ALDEFLUOR reagent and then immediately with ALDH inhibitor DEAB. These cells were used to set the gate for the negative population. FACSCanto II (BD Biosciences) was used for the measurement and data was further analyzed with FCS Express Software (De Novo Software). Each condition was independently repeated 2 times.

Lentivirus preparation and gene knockdown

Previously prepared Lentivector plasmids with shRNA-mediated genes such as AMPKα1, AMPKα2, Ulk1 and ATG5, were cultured in 37°C incubation overnight in a shaker with 200 rpm and isolated using Fast-n-Easy Plasmid Mini-Prep kit protocol. Plasmid mixture was prepared using packaging plasmid psPAX2, envelope plasmid pMD2.G and previously prepared lentivector plasmids for transformation in HEK293 cells using LipoD293 and 100U Pen-strep antibiotic. For nutrient-rich conditions, HEK293 cells were cultured in DMEM medium containing 10% FCS and on the other hand, PC-3M-Pro4 cells were cultured and passaged in DMEM medium containing 10% FC-II. The HEK293 cell suspension containing lentivirus was collected and stored in -80°C. The lentivirus was transfected into PC-3M-Pro4 cells kept in culture (1ml for each knockdown) in presence of 1µg/ml Polybrene (Sigma-Aldrich). After 24h of 37°C incubation, the cells were treated with 1µg/ml of puromycin for selection of properly transfected cells.

Statistics

Statistical analysis was performed with GraphPad Prism 6.0 (San Diego, CA, USA). T-Test was used to compare two groups and ANOVA for multiple groups. The data is presented as mean ±SEM or mean ±SD. P-values ≤0.05 are considered to be statistically significant (*p≤0.05, **p≤0.01, ***p≤0.001, ****p≤0.0001).

Acknowledgement

We thank Dr. Gabriel van der Pluijm (Deportment of Urology, LUMC) for providing experimental material Guido de Roo from the Flow cytometry facility (Department of Hematology, LUMC) for technical support, Prof. Rob Hoeben and Martijn Rabelink (Department of Cell Biology, LUMC) for providing lentiviral shRNA vectors (Sigma-Aldrich). The present work was supported by a personalized medicine grant from Alpe D'HuZes (AdH)/KWF PROPER entitled "Near-patient prostate cancer models for the assessment of disease prognosis. We also would like to thank other lab members Arwin Groenewoud and Quanchi Chen for their help throughout this project .

References

Collins, A. T., Berry, P. A., Hyde, C., Stower, M. J., & Maitland, N. J. (2005). Prospective identification of tumorigenic prostate cancer stem cells. *Cancer Research*, *65*(23), 10946–10951. https://doi.org/10.1158/0008-5472.CAN-05-2018

Dasupta, B., Seibel, W. (2018). Compound C/Dorsomorphin: Its Use and Misuse as an AMPK Inhibitor. *Methods in Molecular Biology*, AMPK pp 195-202. DOI :10.1007/978-1-4939-7598-3_12

Dc, W., Jones, B. Y. R. J., Barber, J. P., Vala, M. S., Collector, M. I., Kaufmann, S. H., … Hilton, J. (2011). Assessment of aldehyde dehydrogenase in viable cells, *10*(10), 2742–2746.

Hanahan, D., & Weinberg, R. A. (2011). Hallmarks of cancer: the next generation. *cell*, *144*(5), 646-674.

Faubert, B., Vincent, E. E., Poffenberger, M. C., & Jones, R. G. (2015). The AMP-activated protein kinase (AMPK) and cancer: Many faces of a metabolic regulator. *Cancer Letters*, *356*(2), 165–170. https://doi.org/10.1016/j.canlet.2014.01.018

Hardie, D. G., Pan, D. A. (2002). Regulation of fatty acid synthesis and oxidation by the AMP-activated protein kinase. *Biochemical Society Transactions, 30*(6), 1064-1070. http://doi.org/10.1042/bst0301064

Hagenbuchner, J., & Ausserlechner, M. J. (2013). Mitochondria and FOXO3: Breath or die. *Frontiers in Physiology*, *4 JUN*(June), 1–10. https://doi.org/10.3389/fphys.2013.00147

Hopkins, T. A., Dyck, J. R. B., Lopaschuk, G. D. (2003). AMP-activated protein kinase regulation of fatty acid oxidation in the ischaemic heart. *Biochemical Society Transactions, 31*(1), 207-212. https://doi.org/10.1042/bst0310207 Integraal kankercentrum Nederland (IKNL). Nederlandse Kankerregistratie. Available from: https://www.cijfersoverkanker.nl/ . [accessed 28th February 2019].

Kabeya, Y. (2004). LC3, GABARAP and GATE16 localize to autophagosomal membrane depending on form-II formation. *Journal of Cell Science*, *117*(13), 2805–2812. https://doi.org/10.1242/jcs.01131

Ke, R., Xu, Q., Li, C., Luo, L., & Huang, D. (2018). Mechanisms of AMPK in the maintenance of ATP balance during energy metabolism. *Cell Biology International*, *42*(4), 384–392. https://doi.org/10.1002/cbin.10915

Kelly, K., & Yin, J. J. (2008). Prostate cancer and metastasis initiating stem cells. *Cell Research*, *18*(5), 528–537. https://doi.org/10.1038/cr.2008.50

Kim, J., Kundu, M., Viollet, B., & Guan, K. L. (2011). AMPK and mTOR regulate autophagy through direct phosphorylation of Ulk1. *Nature Cell Biology*, *13*(2), 132–141. https://doi.org/10.1038/ncb2152

Kumazoe, M., Takai, M., Hiroi, S., Takeuchi, C., Kadomatsu, M., Nojiri, T., … Tachibana, H. (2017). The FOXO3/PGC-1β signaling axis is essential for cancer stem cell properties of pancreatic ductal adenocarcinoma. *Journal of Biological Chemistry*, *292*(26), 10813–10823. https://doi.org/10.1074/jbc.M116.772111

Moreno-Smith, M., Lutgendorf, S. K., & Sood, A. K. (2010). Impact of stress on cancer metastasis. *Future oncology*, *6*(12), 1863-1881.

Labelle, M., & Hynes, R. O. (2013). The initial hours of metastasis: the importance of cooperative host-tumor cell interactions during hematogenous dissemination, *2*(12), 1091–1099. https://doi.org/10.1158/2159-8290.CD-12-0329.The

Liang, R., & Ghaffari, S. (2017). Mitochondria and FOXO3 in stem cell homeostasis, a window into hematopoietic stem cell fate determination. *Journal of Bioenergetics and Biomembranes*, *49*(4), 343–346. https://doi.org/10.1007/s10863-017-9719-7

Martı, A., Aguirre-gamboa, R., Gomez-rueda, H., Martı, E., Chacolla-huaringa, R., & Rodriguez-barrientos, A. (2013). SurvExpress : An Online Biomarker Validation Tool and Database for Cancer Gene Expression Data Using Survival Analysis, *8*(9), 1–9. https://doi.org/10.1371/journal.pone.0074250

Mizushima, N. (2007). Autophagy: process and function. Genes & development, *21*(22), 2861-2873.

Ni, J., Cozzi, P., Hao, J., Graham, P., Li, Y., Kearsley, J., & Duan, W. (2014). Cancer stem cells in prostate cancer chemoresistance. *Current Cancer Drug Targets*, *14*(3), 225–240. https://doi.org/10.2174/1568009614666140328152459

Prasetyanti, P. R., & Medema, J. P. (2017). Intra-tumor heterogeneity from a cancer stem cell perspective. *Molecular Cancer*, *16*(1), 1–9. https://doi.org/10.1186/s12943-017-0600-4

Quintanilla-Vega, B., Burns, M., del Razo, L. M., Khalimonchuk, O., Navarro-Yepes, J., Franco, R., … Anandhan, A. (2014). Oxidative Stress, Redox Signaling, and Autophagy: Cell Death Versus Survival . *Antioxidants & Redox Signaling*, *21*(1), 66–85. https://doi.org/10.1089/ars.2014.5837

Rueden, C. T., Schindelin, J., Hiner, M. C., Dezonia, B. E., Walter, A. E., Arena, E. T., & Eliceiri, K. W. (2017). ImageJ2 : ImageJ for the next generation of scientific image data, 1–26. https://doi.org/10.1186/s12859-017-1934-z

Shiozawa, Y., Pedersen, E. A., Havens, A. M., Jung, Y., Mishra, A., Joseph, J., … Taichman, R. S. (2011). Human prostate cancer metastases target the hematopoietic stem cell niche to establish footholds in mouse bone marrow. *Conflict*, *121*(4). https://doi.org/10.1172/JCI43414DS1

Statz, C. M., Patterson, S. E., & Mockus, S. M. (2017). mTOR inhibitors in castration-resistant prostate cancer: a systematic review. *Targeted oncology*, *12*(1), 47-59.

Zachari, M., & Ganley, I. G. (2017). The mammalian ULK1 complex and autophagy initiation.*Essays In Biochemistry,* 61(6), 585–596. https://doi.org/10.1042/ebc20170021

Supplementary figures

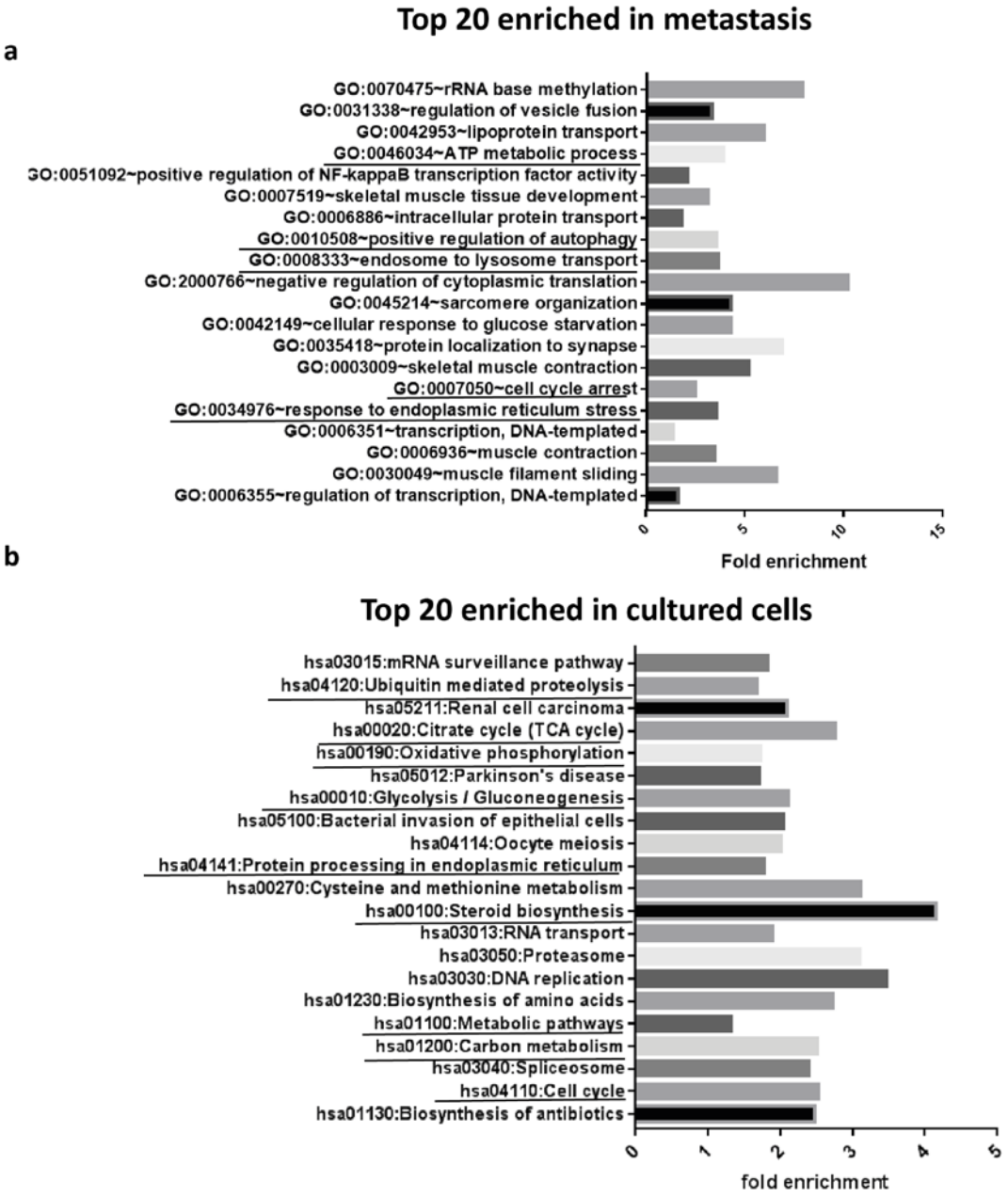

Supplementary Figure. 1 (a-c) PC-3M-Pro4 in zebrafish metastases have enhanced expression of gene signatures for stress coping but reduced expression of genes for metabolic process in comparison with cells in culture. (a) Top 20 most upregulated gene terms in zebrafish metastasis. Terms related to stress response were highlighted. (b) Top 20 most down-regulated gene terms in metastasis. Terms related to metabolisms and cell cycle were highlighted. (c) Gene set enrichment analysis revealed a downregulation of gene signatures for glycolysis and mTORC1. P<0.001.